Efficient and robust coupling of finite element and diffuse field models for sound transmission prediction

E. Reynders
KU Leuven Department of Civil Engineering, Kasteelpark Arenberg 40, B-3001 Leuven, Belgium

Summary
Predicting the airborne or structure-borne sound transmission through a real-life building element generally requires a detailed model of that element. Simplified analytical structural models based on infinite thin plate theory are important for gaining insight into the physical principles of the sound transmission process, but they are inaccurate when the modal behavior of the building element is important or when the geometry of the wall is complex. A commonly adopted strategy therefore consists of constructing a detailed finite element model and computing the expected value of the sound reduction index by numerically integrating the plane-wave transmission over all angles of incidence. This is not only computationally costly, but all information on the uncertainty of the predicted values due to the statistical nature of the diffuse acoustic field model is also lost. An alternative, more efficient method for coupling a finite element model of a building element to diffuse field models of the rooms has been recently presented. It is based on two recent developments in diffuse field theory: a direct field - diffuse field reciprocity relationship and the the Gaussian Orthogonal Ensemble model for the natural frequencies and mode shapes of a diffuse component. Both the mean and variance of the sound reduction index can be computed, so that the uncertainty of the predicted values due to the diffuse acoustic field assumption can be assessed. In this paper, the method is employed for predicting the sound transmission through complex building elements. The predictions are validated against available measurement data, and it is found that the proposed approach can capture both the complex dynamics of the walls and the uncertainty that is related with the diffuse acoustic field assumption.

PACS no. 43.55.Rg, 43.55.Ti, 43.55.Nd, 43.40.Hb

1. Introduction

Predicting the airborne or structure-borne sound transmission through a real-life building element generally requires a detailed model of that element. Simplified analytical structural models based on infinite thin plate theory are very important for gaining insight into the physical principles of the sound transmission process, but they are inaccurate when the modal behavior of the building element is important or when the geometry of the wall is complex [1, 2]. A commonly adopted strategy therefore consists of constructing a detailed finite element (FE) model and computing the expected value of the sound reduction index by numerically integrating the plane-wave transmission over all angles of incidence. This is not only computationally costly, but all information on the uncertainty of the predicted values due to the statistical nature of the diffuse acoustic field model is also lost.

An alternative, more efficient method for coupling a finite element model of a building element to diffuse field models of the rooms has been recently developed [3, 4, 5]. It is based on two recent developments in diffuse field theory: a direct field - diffuse field reciprocity relationship [6] and the the Gaussian Orthogonal Ensemble model for the natural frequencies and mode shapes of a diffuse component [7]. Both the mean and variance of the sound reduction index can be computed, so that the uncertainty of the predicted values due to the diffuse acoustic field assumption can be assessed. The method is also known as the hybrid finite element - statistical energy analysis (FE-SEA) method, however, it is much more general than standard SEA because coupling loss factors can be computed in a logically consistent and straight forward way, also when the overall system contains deterministic components [8], and because correct vari-

ance values, representing the uncertainty inherent in the diffuse field assumption, can also be obtained [4]. This paper provides a brief overview of the hybrid FE-diffuse field method and recent applications and validations towards predicting the sound transmission through building elements of increasing complexity. More details can be found in [9, 10].

2. Hybrid finite element - diffuse field modeling

In this section, the hybrid method is introduced by means of an example situation, where a finite element model of a wall is coupled to two diffuse sound field models of the adjoining rooms. A general setting of the method can be found in [5, 9].

2.1. Notations and definitions

The response degrees of freedom (DOFs) at pulsation ω of the wall are collected in an amplitude vector $\mathbf{q} \in \mathbb{C}^{N_{\text{dof}}}$, so that the time-domain response of the wall is given by $\text{Re}(\mathbf{q}e^{i\omega t})$. Similarly, the external harmonic loads at ω applied at these degrees of freedom are collected in the load amplitude vector $\mathbf{f} \in \mathbb{C}^{N_{\text{dof}}}$. The equations of motion of the complete system (wall and rooms) are then

$$\mathbf{D}\mathbf{q} = \mathbf{f}, \tag{1}$$

where $\mathbf{D} \in \mathbb{C}^{N_{\text{dof}} \times N_{\text{dof}}}$ denotes the dynamic stiffness matrix at frequency ω. $\mathbf{D}$ is a random matrix because it represents the dynamic behavior of the overall system, including the diffuse sound fields, at the wall DOFs. It may be decomposed as the sum of the dynamic stiffness matrix of the wall, denoted as $\mathbf{D}_{\text{d}}$, and the dynamic stiffness matrices of the two sound fields, denoted as $\mathbf{D}_1$ and $\mathbf{D}_2$:

$$\mathbf{D} = \mathbf{D}_{\text{d}} + \mathbf{D}_1 + \mathbf{D}_2. \tag{2}$$

The dynamic stiffness matrix of a diffuse sound field is decomposed as

$$\mathbf{D}_k = \mathbf{D}_{\text{dir}}^{(k)} + \mathbf{D}_{\text{ran}}^{(k)}, \tag{3}$$

where $\mathbf{D}_{\text{dir}}^{(k)}$ denotes the mean of the dynamic stiffness matrix: $\mathbf{D}_{\text{dir}}^{(k)} := \text{E}\left[\mathbf{D}_k\right]$. With this decomposition, the equations of motion for a diffuse sound field can be written as

$$\mathbf{D}_{\text{dir}}^{(k)}\mathbf{q} = \mathbf{f}_k + \mathbf{f}_{\text{ran}}^{(k)}, \tag{4}$$

where the *reverberant forces* are defined as $\mathbf{f}_{\text{ran}}^{(k)} := -\mathbf{D}_{\text{ran}}^{(k)}\mathbf{q}$, and $\mathbf{f}_k$ denotes the sum of the loads applied to sound field k at the wall DOFs. The overall equations of motion (1) become

$$\mathbf{D}_{\text{tot}}\mathbf{q} = \mathbf{f} + \mathbf{f}_{\text{ran}}^{(1)} + \mathbf{f}_{\text{ran}}^{(2)}, \tag{5}$$

where $\mathbf{D}_{\text{tot}} := \mathbf{D}_{\text{d}} + \mathbf{D}_{\text{dir}}^{(1)} + \mathbf{D}_{\text{dir}}^{(2)}$ is purely deterministic because it is the mean of the dynamic stiffness matrix of the overall system: $\mathbf{D}_{\text{tot}} = \text{E}\left[\mathbf{D}\right]$.

2.2. Mean harmonic response

The mean total energy $\hat{E}_j$ of each random sound field j can be obtained from a stationary power balance which involves the other random sound fields as well as the deterministic wall [3]. For the special case where the external loading acts on the sound fields but not on the wall in between, this reads:

$$\begin{aligned} \text{E}[P_1] &= \omega\left(\eta_1 + \eta_{\text{d},1}\right)\hat{E}_1 + \omega\eta_{12}n_1\left(\frac{\hat{E}_1}{n_1} - \frac{\hat{E}_2}{n_2}\right) \\ \text{E}[P_2] &= \omega\left(\eta_2 + \eta_{\text{d},2}\right)\hat{E}_2 + \omega\eta_{21}n_2\left(\frac{\hat{E}_2}{n_2} - \frac{\hat{E}_1}{n_1}\right) \end{aligned} \tag{6}$$

In this expression, η_j is the damping loss factor of sound field j, n_j its modal density, P_j the power input from external forces applied directly to this subsystem, and

$$\omega\eta_{\text{d},j} = \frac{2}{\pi n_j}\sum_{r,s}\text{Im}\left(D_{\text{d},rs}\right)\left(\mathbf{D}_{\text{tot}}^{-1}\text{Im}\left(\mathbf{D}_{\text{dir}}^{(j)}\right)\mathbf{D}_{\text{tot}}^{-H}\right)_{rs} \tag{7}$$

$$\omega\eta_{jk}n_j = \frac{2}{\pi}\sum_{r,s}\text{Im}\left(D_{\text{dir},rs}^{(j)}\right)\left(\mathbf{D}_{\text{tot}}^{-1}\text{Im}\left(\mathbf{D}_{\text{dir}}^{(k)}\right)\mathbf{D}_{\text{tot}}^{-H}\right)_{rs} \tag{8}$$

where the superscript ^{H} denotes Hermitian transpose. Since both sound fields are weakly coupled through the wall, $\text{E}[P_j]$ can be approximated as the power input to the mean uncoupled subsystem. It can be noted that the power balance equation (6) has the same structure as in conventional SEA. Therefore the factors η_{jk} represent coupling loss factors, and (8) provides a rigorous and straightforward way to compute them, even when the overall vibro-acoustic system contains purely deterministic components. The coupling loss factors, as computed from (8), automatically contain the effects of both resonant and non-resonant transmission, while in conventional SEA, these effects need to be considered separately [8].

The frequency-dependent matrix $\mathbf{D}_{\text{dir}}^{(k)}$ of each sound field can be computed as its the direct field receptance matrix [11, 8]. The term 'direct field' denotes the part of the room response containing incoming waves only; it is the limiting response that would be observed at the interface with the wall when the extent of the room would be increased towards infinity. The direct field dynamic stiffness matrix of a room as seen by the wall therefore corresponds to the one of a grid of points covering the interface between the room and the wall, but embedded in an infinite planar baffle.

2.3. Variance of the harmonic response

For the computation of the variance of the total energy of each sound field in the considered situation, the interested reader is referred to [9, Sec. 2.3].

2.4. Sound reduction index

In laboratory conditions, the sound reduction index R is determined from the following measurement formula:

$$R = L_{p1} - L_{p2} + 10\log\frac{S}{A_2}, \tag{9}$$

where L_{p1} and L_{p2} are the spatially averaged stationary sound pressure levels in the emitting and receiving rooms, respectively, S is the surface area of the partition and A_2 the absorption of the receiving room. In stationary conditions, the total energy of a subsystem, consisting of the sum the kinetic and potential energies, is constant. For low damping and at resonance, the kinetic and potential energies at a particular nonzero frequency will be approximately equal [12]. An equivalent expression for (9) is therefore [9]

$$R = 10\log\frac{E_1 V_2 S}{E_2 V_1 A_2}, \tag{10}$$

where E_1 and E_2 represent the total energy in the emitting and receiving rooms, respectively, and V_1 and V_2 their respective volumes. A first-order Taylor expansion of (10) around $R = 10\log\left(\hat{E}_1 V_2 S/\left(\hat{E}_2 V_1 A_2\right)\right)$ can be analytically computed, resulting in the following approximations for the mean

$$\mathrm{E}[R] \approx 10\log\frac{\hat{E}_1 V_2 S}{\hat{E}_2 V_1 A_2}, \tag{11}$$

and variance

$$\sigma_R^2 \approx \frac{100}{\ln^2(10)}\left(\frac{\mathrm{Var}(E_1)}{\hat{E}_1^2} - \frac{2}{\hat{E}_1\hat{E}_2}\mathrm{Cov}(E_1,E_2) + \frac{\mathrm{Var}(E_2)}{\hat{E}_2^2}\right) \tag{12}$$

of the sound reduction index [9].

3. Applications and experimental validation

In this section, the capabilities of the hybrid method for predicting the sound transmission through building elements is illustrated for recently reported applications on wall systems of increasing complexity. The hybrid model predictions are compared with measurements, performed in the transmission suite of the Laboratory of Acoustics of KU Leuven. The rooms of this transmission suite each have a volume of 87 m^3. The air density, sound speed and reverberation time of the rooms are taken to be constant with values of $\rho_a = 1.20$ $\mathrm{kg/m}^3$, $c = 343$ m/s and $T = 1.5$ s, respectively.

3.1. Rib-stiffened plate

The first structure is a rib-stiffened PMMA plate of dimensions 1.25 m × 1.5 m × 15 mm, to which 11 steel L30 stiffeners with a length of 1.395m are attached (Fig. 1). The center-to-center spacing between the stiffeners is 100 mm, the distance between a vertical edge of the plate and a vertical edge of the closest stiffener is 110 mm, and the distance between a horizontal edge of the plate and the closest end section of a stiffener is 52.5 mm. The stiffeners are both glued to the base plate over their entire length, and additionally screwed to the base plate at four points.

Figure 1. PMMA plate with 11 steel L30 stiffeners attached.

A finite element (FE) model of the structure was made using the commercial software ANSYS [10]. The base plate was modeled with four-node shell elements and the stiffeners were modeled with two-node Timoshenko beam elements. The plate and the stiffeners were fully coupled, and the offset of the stiffeners with respect to the midplane of the plate taken into account. Simply supported boundary conditions were applied at all edges of the plate. For the steel profiles, a Young's modulus of $E_\mathrm{s} = 210$ GPa, Poisson's ratio of $\nu_\mathrm{s} = 0.3$ and density of $\rho_\mathrm{s} = 7850$ $\mathrm{kg/m}^3$ were taken. The material properties of the PMMA base plate were estimated at $E_\mathrm{p} = 5.125$ GPa, $\nu_\mathrm{p} = 0.35$ and $\rho_\mathrm{p} = 1170$ $\mathrm{kg/m}^3$.

The structural finite element model is coupled to a GOE diffuse model of the rooms using the hybrid method. The predicted sound reduction index (mean and 95 % confidence interval), is plotted in Fig. 2 together with the measured values which were averaged

over 1/48-octave bands. The measured R fluctuates around the mean prediction and the measured fluctuations lie nearly always within the predicted 95 % confidence interval. At the lowest frequencies, this confidence interval is very wide, thus indicating that the hybrid model predictions (with diffuse field models for the sound fields in the rooms) are not adequate at those frequencies. However, the uncertainty decreases rapidly with frequency, so that from about 125 Hz onwards, useful conclusions can be drawn from the model.

The pronounced dips that are observed in both the measured and the predicted sound reduction index above 140 Hz correspond with some of the eigenfrequencies of the finite-sized rib-stiffened plate. They do not correspond with eigenfrequencies of the bare rooms, as these are not included in the hybrid FE-SEA model. The dips can be attributed to a discrete coincidence phenomenon which involves only specific plate modes, namely, those modes for which the total wave number is close the the free-field acoustic wave number at the same frequency [10].

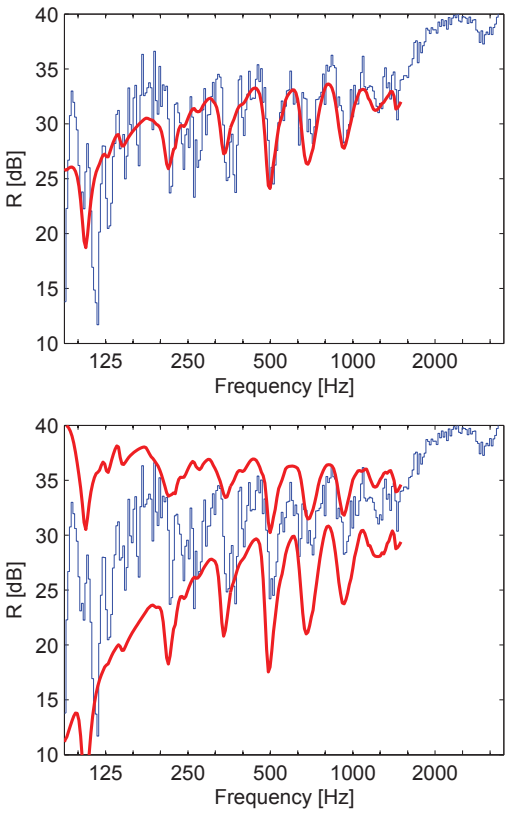

Figure 2. Measured sound reduction index of a rib-stiffened plate in 1/48-octave bands (blue) vs. the harmonic mean values (red, top) and 95 % confidence intervals (red, bottom) as predicted with the hybrid method.

3.2. Lightweight perforated brick wall

The second structure is a perforated brick wall, plastered at both sides, of dimensions 3.25 m × 1.95 m × 0.19 m. The acoustic behavior of perforated brick walls is complex, given the inhomogeneities at three different scales: that of the fire clay material, that of the brick where small cavities are present in the fire clay because of the perforations, and that of the complete wall where the bricks are held together by mortar layers. When the inhomogeneities are small compared to the wavelength, and when the stiffness is only slightly different in all directions, the wall can be modeled as homogeneous and isotropic. The thickness effects, however, can not be neglected: not only is shear deformation important, thickness resonances (i.e., Lamb modes) are often observed as well in the audio frequency range [13]. Therefore, a 3D finite element model of the wall is made in ANSYS using volume (solid) elements. The boundary displacements in the middle plane are restrained. Following [14], the equivalent Young's modulus, Poisson's ratio, density and thickness are taken to be $E = 1825$ MPa, $\nu = 0.2$, $\rho = 613.5$ kg/m^3 and $t = 0.2934$ m, respectively.

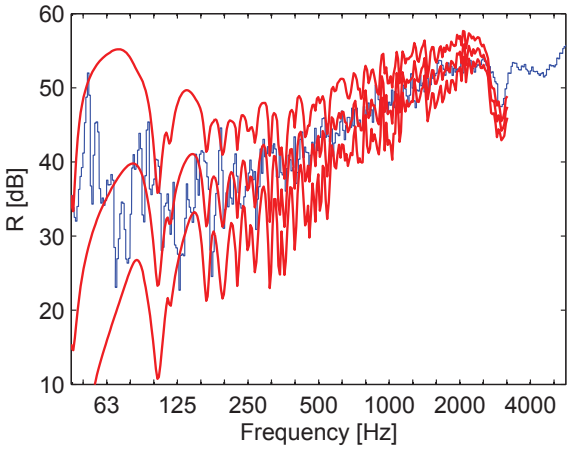

Figure 3. Sound transmission loss of a lightweight perforated brick wall. Predicted mean and 95 % confidence interval, computed with the hybrid method (red), vs. laboratory measurements (blue).

The sound reduction index predicted with the hybrid method (mean and 2σ confidence interval), is plotted in Fig. 3 together with the measured values reported in [14] which are averaged over 1/48-octave bands. Individual resonance dips of the wall are very clearly visible in the predicted sound reduction index because of the high stiffness and low damping of the wall. Another clear dip, which is caused by the first thickness resonance of the wall, is visible around 3000 Hz. The width of the confidence interval decreases slowly with frequency. The uncertainty accounted for in the model can for a large part explain the discrepancies between measurements and model

predictions from about 125 Hz onwards, i.e., in the mid-frequency range.

3.3. Double glazing

The final structure consists of two glass panes, 6 mm and 8 mm thick, separated by an air cavity of 12 mm. The dimensions are 1.20 m×1.45 m. As material properties of the glass, a density of $\rho = 2500$ kg/m^3, a modulus of elasticity of $E = 62$ GPa, and a Poisson's ratio of $\nu = 0.24$ are taken. For the damping loss factor of the glass panes, measured values are used, while the air cavity is taken to be undamped.

The glazing is modeled with a Rayleigh-Ritz approach, where the analytic modes of the decoupled simply supported glass panes and the decoupled hard-walled cavity are taken as Ritz basis vectors (see [15, App.] for details). This deterministic wall model is then coupled to the nonparametric stochastic models of the rooms with the hybrid method, and the sound transmission loss is computed.

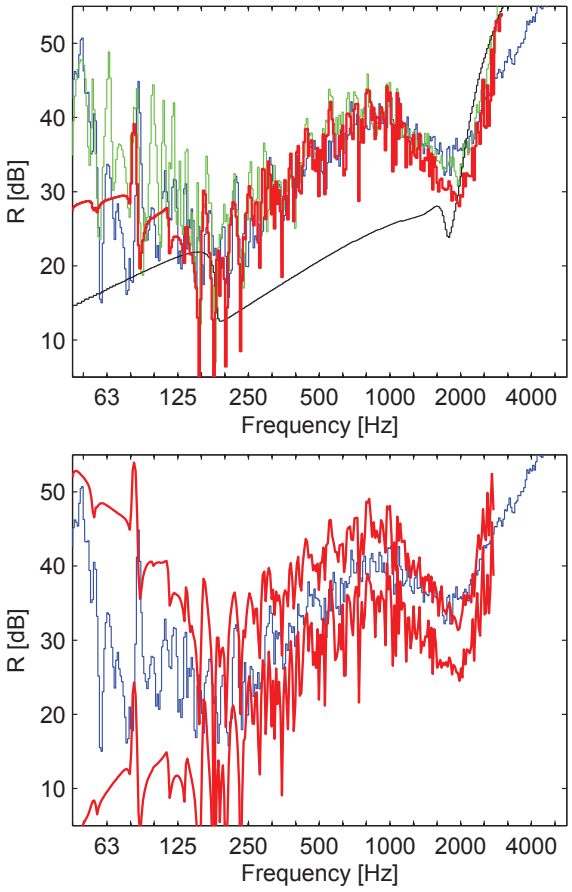

Figure 4. Sound transmission loss of double glazing 6−12−8 mm. (top) Predicted mean, computed with the hybrid method (red), vs. laboratory measurements (blue) and deterministic predictions with the TMM (black) and WBM (green) methods. (bottom) 2σ confidence interval of the hybrid model predictions (red) vs. laboratory measurements (blue).

The mean of the computed sound transmission loss is plotted in Fig. 4 together with the 2σ confidence interval. Individual resonance dips of the glazing are very clearly visible in the hybrid model predictions because of the high stiffness of the glass panes and the low damping (the air cavity was taken to be undamped). A dip in the transmission loss is also visible around 186.5 Hz which corresponds with the mass-spring-mass resonance frequency of the glass panes on the thin air layer when the plane dimensions of the glazing would be extended towards infinity. Measured values, averaged over 1/48-octave bands, are also shown. An excellent correspondence between the measured and predicted values is observed, except at the highest frequencies, where flanking transmission between both glass panes could affect the measured sound reduction index, while this effect has not been included in any of the models.

In Fig. 4, the measurements and hybrid model predictions are also compared with the corresponding values obtained with two deterministic methods: the transfer matrix method (TMM) and the wave-based method (WBM). The transfer matrix method [16] models the double glazing as consisting of infinite layers of glass and air and the adjacent rooms as infinite half spaces with diffuse sound field. This method largely underestimates the transmission loss between the mass-spring-mass resonance frequency of the glazing and the coincidence frequency. As discussed in [17], this cannot be resolved by applying correction terms for the diffraction effects by spatially windowing the results or a Gaussian distribution of incident energy. This illustrates that, for double walls, it is important to take the modal behavior of the finite partition structure into account in this broad frequency range. The wave-based method [18, 19] is a deterministic method that takes the modal behavior of both the rooms and the glazing into account. It shows a very good agreement with the measured data, but it requires a much larger computational effort than the hybrid method as the rooms need to be modeled with a large number of degrees of freedom (fundamental wave solutions), and it does not provide information on the uncertainty caused by small variations in the acoustic mass and stiffness distributions, which have a wave scattering effect.

4. Conclusions

A stochastic method for vibro-acoustic analysis, consisting of a hybridization of deterministic and diffuse field modeling, has been recently developed. Compared to fully deterministic methods such as finite element analysis or the wave-based method, the method is computationally very cheap, since subsystems that carry a diffuse field are characterized by a single degree of freedom: the total energy. In this paper, the focus has been on the sound transmission through a

complex wall that is situated in between two rooms, each of which having a diffuse sound field. Not only mean values of the sound reduction index, but also variances, that are inherent to the adopted random wave scattering model underlying the diffuse field assumption, were obtained. Predictions have been validated against measurements, and it was found that the proposed approach can capture both the complex dynamics of the walls and the uncertainty of the generalized diffuse field assumption of the acoustic fields.

Acknowledgement

This research has been supported through a Postdoctoral Fellowship of the Research Foundation Flanders (FWO) and an Assistant Professorship at KU Leuven. The financial support of FWO and KU Leuven is gratefully acknowledged.

References

[1] C. Hopkins, Sound insulation, Elsevier Ltd., Oxford, 2007.

[2] T. Vigran, Building Acoustics, Taylor & Francis, Oxon, UK, 2008.

[3] P. Shorter, R. Langley, Vibro-acoustic analysis of complex systems, Journal of Sound and Vibration 288 (3) (2005) 669–699.

[4] R. Langley, V. Cotoni, Response variance prediction for uncertain vibro-acoustic systems using a hybrid deterministic-statistical method, Journal of the Acoustical Society of America 122 (6) (2007) 3445–3463.

[5] E. Reynders, R. Langley, Response probability distribution of built-up vibro-acoustic systems, Journal of the Acoustical Society of America 131 (2) (2012) 1138–1149.

[6] R. Langley, On the diffuse field reciprocity relationship and vibrational energy variance in a random subsystem at high frequencies, Journal of the Acoustical Society of America 121 (2) (2007) 913–921.

[7] E. Reynders, J. Legault, R. Langley, A probabilistic approach to the vibro-acoustic analysis of built-up systems based on the Gaussian Orthogonal Ensemble, Journal of the Acoustical Society of America 136 (1) (2014) 201–212.

[8] R. Langley, J. Cordioli, Hybrid deterministic-statistic analysis of vibro-acoustic systems with domain couplings on statistical components, Journal of Sound and Vibration 321 (3–5) (2009) 893–912.

[9] E. Reynders, R. Langley, A. Dijckmans, G. Vermeir, A hybrid finite element - statistical energy analysis approach to robust sound transmission modelling, Journal of Sound and Vibration 333 (19) (2014) 4621–4636.

[10] E. Reynders, C. Van hoorickx, An investigation into the sound insulation of finite-sized rib-stiffened plates, in: Proceedings of 7th Forum Acusticum, Kraków, Poland, 2014, cD-ROM.

[11] P. Shorter, R. Langley, On the reciprocity relationship between direct field radiation and diffuse reverberant loading, Journal of the Acoustical Society of America 117 (1) (2005) 85–95.

[12] L. Cremer, M. Heckl, B. Petersson, Structure-borne sound: Structural vibrations and sound radiation at audio frequencies, 3rd Edition, Springer, Berlin, 2005.

[13] G. Jacqus, S. Berger, V. Gibiat, P. Jean, M. Villot, S. Ciukay, A homogenised vibratory model for predicting the acoustic properties of hollow brick walls, Journal of Sound and Vibration 330 (14) (2011) 3400–3409.

[14] A. Dijckmans, Wave based calculation methods for sound-structure interaction: application to sould insulation and sound radiation of composite walls and floors, Ph.D. thesis, KU Leuven (2011).

[15] E. Reynders, Parametric uncertainty quantification of sound insulation values, Journal of the Acoustical Society of America 135 (4) (2014) 1907–1918.

[16] W. Lauriks, P. Mees, J. F. Allard, The acoustic transmission through layered systems, Journal of Sound and Vibration 155 (1) (1992) 125–132.

[17] A. Dijckmans, G. Vermeir, W. Lauriks, Sound transmission through finite lightweight multilayered structures with thin air layers, Journal of the Acoustical Society of America 128 (6) (2010) 3513–3524.

[18] W. Desmet, B. van Hal, P. Sas, D. Vandepitte, A computationally efficient prediction technique for the steady-state dynamic analysis of coupled vibro-acoustic systems, Advances in Engineering Software 33 (2002) 527–540.

[19] B. Pluymers, B. van Hal, D. Vandepitte, W. Desmet, Trefftz-based methods for time-harmonic acoustics, Archives of Computational Methods in Engineering 14 (4) (2007) 343–381.